

## APPLIED SCIENCES AND ENGINEERING

# Full-color active-matrix organic light-emitting diode display on human skin based on a large-area MoS<sub>2</sub> backplane

Minwoo Choi<sup>1\*</sup>, Sa-Rang Bae<sup>2\*</sup>, Luhing Hu<sup>1</sup>, Anh Tuan Hoang<sup>1</sup>,  
Soo Young Kim<sup>2†</sup>, Jong-Hyun Ahn<sup>1†</sup>

Electronic applications are continuously developing and taking new forms. Foldable, rollable, and wearable displays are applicable for human health care monitoring or robotics, and their operation relies on organic light-emitting diodes (OLEDs). Yet, the development of semiconducting materials with high mechanical flexibility has remained a challenge and restricted their use in unusual format electronics. This study presents a wearable full-color OLED display using a two-dimensional (2D) material-based backplane transistor. The 18-by-18 thin-film transistor array was fabricated on a thin MoS<sub>2</sub> film that was transferred to Al<sub>2</sub>O<sub>3</sub> (30 nm)/polyethylene terephthalate (6 μm). Red, green, and blue OLED pixels were deposited on the device surface. This 2D material offered excellent mechanical and electrical properties and proved to be capable of driving circuits for the control of OLED pixels. The ultrathin device substrate allowed for integration of the display on an unusual substrate, namely, a human hand.

## INTRODUCTION

Rapid developments in the electronic device industry have progressed beyond the improvement of conventional device performance and are maximizing user convenience by integrating various functional features into smart electronic systems (1–3). The development of these types of devices has required extensive research in the field of wearable electronics, where the focus is on rollable and foldable device formats and ultrathin flexible substrates produced using low-temperature processes (e.g., transfer and inkjet printing) (4–6). Inherent limitations in the mechanical and electronic properties of these materials have motivated the use of alternative semiconductor materials. Two-dimensional (2D) semiconducting materials, including MoS<sub>2</sub>, WS<sub>2</sub>, MoSe<sub>2</sub>, and WSe<sub>2</sub>, can be used to incorporate thin-film transistors (TFTs) and logic circuits on ultrathin plastic substrates with relatively high performance (7, 8). These materials are classified as transition metal dichalcogenides and provide unique electrical, optical, and mechanical properties suitable for use in the backplane circuitry of wearable electronics (9, 10). The excellent band gap properties of MoS<sub>2</sub> have led to its application as a switching device in wearable applications (11). Notably, a single-color organic light-emitting diode (OLED) display integrated with MoS<sub>2</sub> backplane circuitry was recently developed (12). While the powerful capabilities of MoS<sub>2</sub> transistors have been demonstrated, notable strides must be made toward achieving highly sophisticated control of red, green, and blue (RGB) colors across a large area, as this is a fundamental and essential requirement of most practical display applications (13–16).

This study aimed to develop a large-area MoS<sub>2</sub> TFT array for the stable operation of 324 pixels in a 2-inch RGB OLED, where the full-color OLED display was demonstrated in an active-matrix con-

figuration. The backplane TFTs were specifically designed to control each color pixel because the RGB OLEDs were made of different organic materials with different optoelectronic characteristics, including luminous efficiency (17). The OLED shows promise for use as a wearable display that can be stably operated on human skin without adverse effects on its optical properties. While previous reports have focused on 2D material-based devices based on homogeneous systems (18, 19), this study demonstrated the potential for fully formed optoelectronic devices with heterogeneous material designs. Wearable full-color OLED displays produced from other classes of 2D material technologies in optoelectronics and wearable devices could be further explored (20).

## RESULTS

A large-area active-matrix OLED (AMOLED) display with a MoS<sub>2</sub> backplane was produced via a sequence of processes, including forming a TFT array on a thin MoS<sub>2</sub> film, depositing an RGB OLED on the drain electrode of the TFTs, peeling the display from the carrier substrate, and transferring the display to the target substrate (e.g., human hand) (Fig. 1A and fig. S1). A bilayer MoS<sub>2</sub> film was synthesized on a 4-inch SiO<sub>2</sub>/Si wafer via metalorganic chemical vapor deposition (MOCVD), which allows for precise control of the gas precursors (9, 21). A polyethylene terephthalate (PET) substrate (6 μm) was coated with Al<sub>2</sub>O<sub>3</sub> (30 nm) using atomic layer deposition (ALD). The MoS<sub>2</sub> film was transferred from the SiO<sub>2</sub>/Si wafer to the PET substrate, producing a MoS<sub>2</sub> transistor array with a driving backplane configuration. The structure of the TFT device was unique, as it was encapsulated with Al<sub>2</sub>O<sub>3</sub> grown by ALD for improved metal contact and carrier mobility due to the n-doping effect in the contact and channel regions (Fig. 1A) (13).

A full-color AMOLED display was produced by depositing RGB OLEDs on the large-area MoS<sub>2</sub> transistor array, which uniformly controls the RGB OLED pixels (Fig. 1A). A schematic illustration and digital photograph of the RGB OLED pixels integrated with the MoS<sub>2</sub> transistors and the full-color AMOLED display placed on a

Copyright © 2020  
The Authors, some  
rights reserved;  
exclusive licensee  
American Association  
for the Advancement  
of Science. No claim to  
original U.S. Government  
Works. Distributed  
under a Creative  
Commons Attribution  
NonCommercial  
License 4.0 (CC BY-NC).

<sup>1</sup>School of Electrical and Electronic Engineering, Yonsei University, Seoul 03722, Republic of Korea. <sup>2</sup>Department of Materials Science and Engineering, Korea University, Seoul 02841, Republic of Korea.

\*These authors contributed equally to this work.

†Corresponding author. Email: sooyoungkim@korea.ac.kr (S.Y.K.); ahnj@yonsei.ac.kr (J.-H.A.)

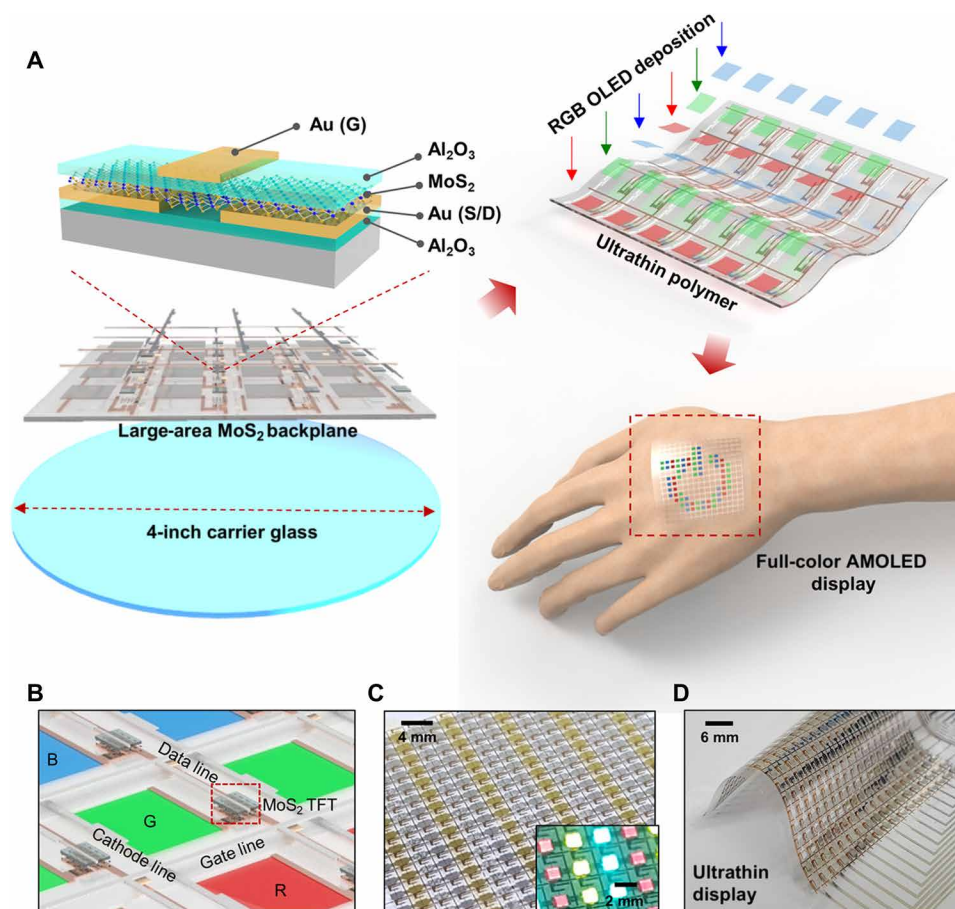


**Fig. 1. The full-color AMOLED display with large-area MoS<sub>2</sub>-based backplane.** (A) Schematic illustration of the high-performance MoS<sub>2</sub>-based backplane on a 4-inch carrier glass substrate, where an Al<sub>2</sub>O<sub>3</sub> capping layer was applied for n-doping effects on the MoS<sub>2</sub> film (top left), an active-matrix full-color display was applied to the ultrathin polymer substrate (top right), and the large-area full-color display was tested on a human hand (bottom right). (B) Scheme of the active-matrix full-color pixel array integrated with MoS<sub>2</sub> transistors, where each pixel was connected via a gate, data, and cathode interconnector for line-addressing control. (C) Digital photograph of the active-matrix display on the 4-inch carrier glass substrate, where the inset demonstrates the full-color display when switched on. (D) Digital photograph of the large-area full-color display on the ultrathin polymer substrate, demonstrating the flexible mechanical properties due to the low bending stiffness of the ultrathin material. Photo credit: Minwoo Choi, Yonsei University.

carrier glass substrate are given in Fig. 1 (B and C). Each pixel was connected to a data and a scanning line, and the entire display circuitry operated in an active-matrix manner. The pixel current was precisely controlled according to the drain and gate signals of the transistor, thereby changing the brightness of the OLED. The inset in Fig. 1C depicts the array operation properties of the active-matrix pixels achieved via line-addressing control. The beneficial mechanical properties associated with an ultrathin display (<7 μm) allowed for stable transfer of the detached device from the carrier glass substrate to a curved surface (e.g., a human hand) without device degradation (Fig. 1, A and D). The mechanical stiffness decreased with decreasing total thickness, which included the device layer and substrate, to improve the mechanical flexibility of the device (22).

The mobility of the MoS<sub>2</sub> transistor was ca.  $18 \pm 10 \text{ cm}^2 \text{ V}^{-1} \text{ s}^{-1}$  at a drain voltage ( $V_{\text{DS}}$ ) of 1 V and on/off ratio above  $10^7$ , as these conditions promoted the doping effects of the Al<sub>2</sub>O<sub>3</sub>-sandwiched structure. The threshold voltage ( $V_{\text{th}}$ ) was  $5 \pm 2 \text{ V}$ , indicating that the pixel was switched off when the gate voltage ( $V_{\text{GS}}$ ) was 0 V, and variation of threshold voltage under negative/positive bias stress was not serious (Fig. 2A and fig. S2). The output curves were evaluated

to determine the drain characteristics of the TFTs (Fig. 2B). There was no drain current ( $I_{\text{DS}}$ ) when the  $V_{\text{GS}}$  was lower than the  $V_{\text{th}}$ , but the current increased with increasing  $V_{\text{GS}}$  at values above the  $V_{\text{th}}$ . The slope of the curve was equal to the conductance of the device and increased linearly with  $V_{\text{GS}}$ , and the extrinsic current ( $I_{\text{DS}}$ ) performance improved when the voltage increased from 4 to 7 V. These characteristics illustrated the relationship between the  $I_{\text{DS}}$  and the bias voltages ( $V_{\text{DS}}$  and  $V_{\text{GS}}$ ). The field effect mobility ( $\mu$ ) histogram indicated an average mobility ( $\mu_{\text{avg}}$ ) of  $18 \text{ cm}^2 \text{ V}^{-1} \text{ s}^{-1}$  across the 324 sample devices (Fig. 2C). Homogeneity of the MOCVD-grown MoS<sub>2</sub> film enables the formation of MoS<sub>2</sub> TFT array with high uniformity, which is necessary for stable display application (figs. S3 and S4). The  $\mu$  of the MoS<sub>2</sub> was appropriate for use as active layer in TFT. Before the operation of a large-area full-color AMOLED display, the performance of a single RGB OLED pixel on the MoS<sub>2</sub> TFT was measured (Fig. 2, D to F, and fig. S5). The turn-on voltages of the three pixels at  $1 \text{ cd/m}^2$  were all ca. 7 V. The luminance increased linearly, and the luminance value of each device was higher than  $500 \text{ cd/m}^2$  at 10 V. The device properties were consistent across all of the samples, and the efficiency did not decrease, confirming

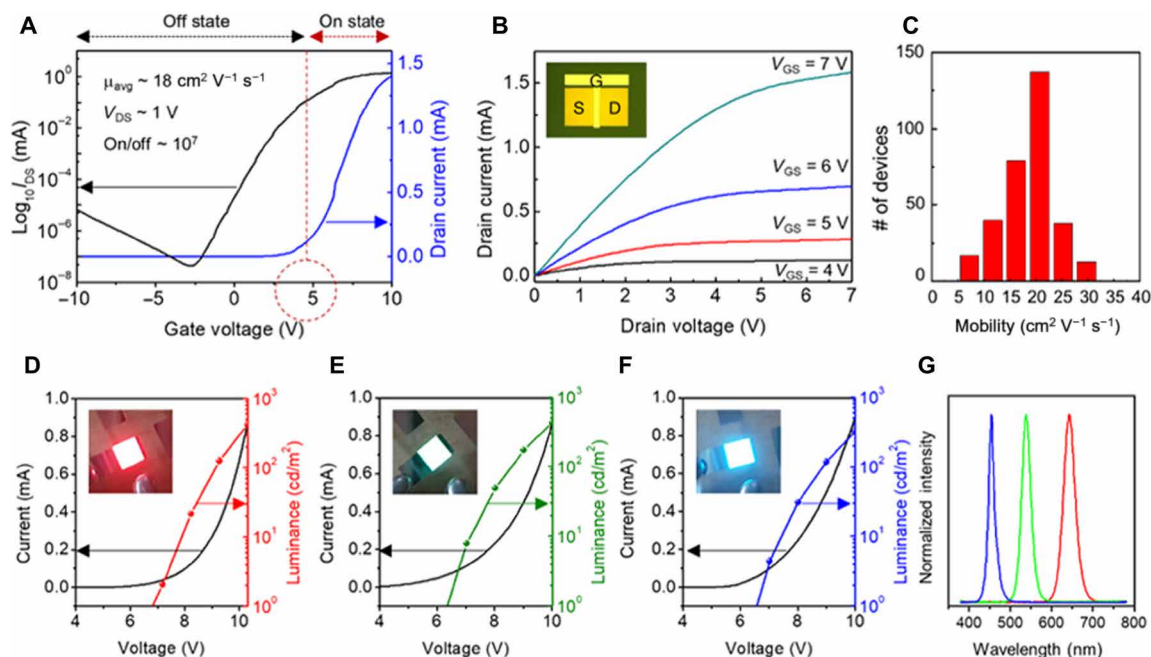


**Fig. 2. Device properties of the MoS<sub>2</sub> transistor and RGB OLEDs.** (A) Transfer curve of the MoS<sub>2</sub> transistor on the 4-inch carrier glass substrate, where the average mobility of  $18 \text{ cm}^2 \text{ V}^{-1} \text{ s}^{-1}$  was sufficient for operating the RGB OLEDs. (B) *I*-*V* characteristics of the MoS<sub>2</sub> transistor as the gate bias was increased from +4 to 7 V, where the inset shows the MoS<sub>2</sub> transistor. (C) Statistical analysis of the MoS<sub>2</sub> transistor mobility across 324 samples. (D to F) *I*-*V* characteristics (left y axis) and luminance (right y axis) of the RGB OLED as a function of applied bias, where the insets visualize the emission of each OLED color. (G) EL spectra of the RGB OLED pixels. Photo credit: Sa-Rang Bae, Korea University.

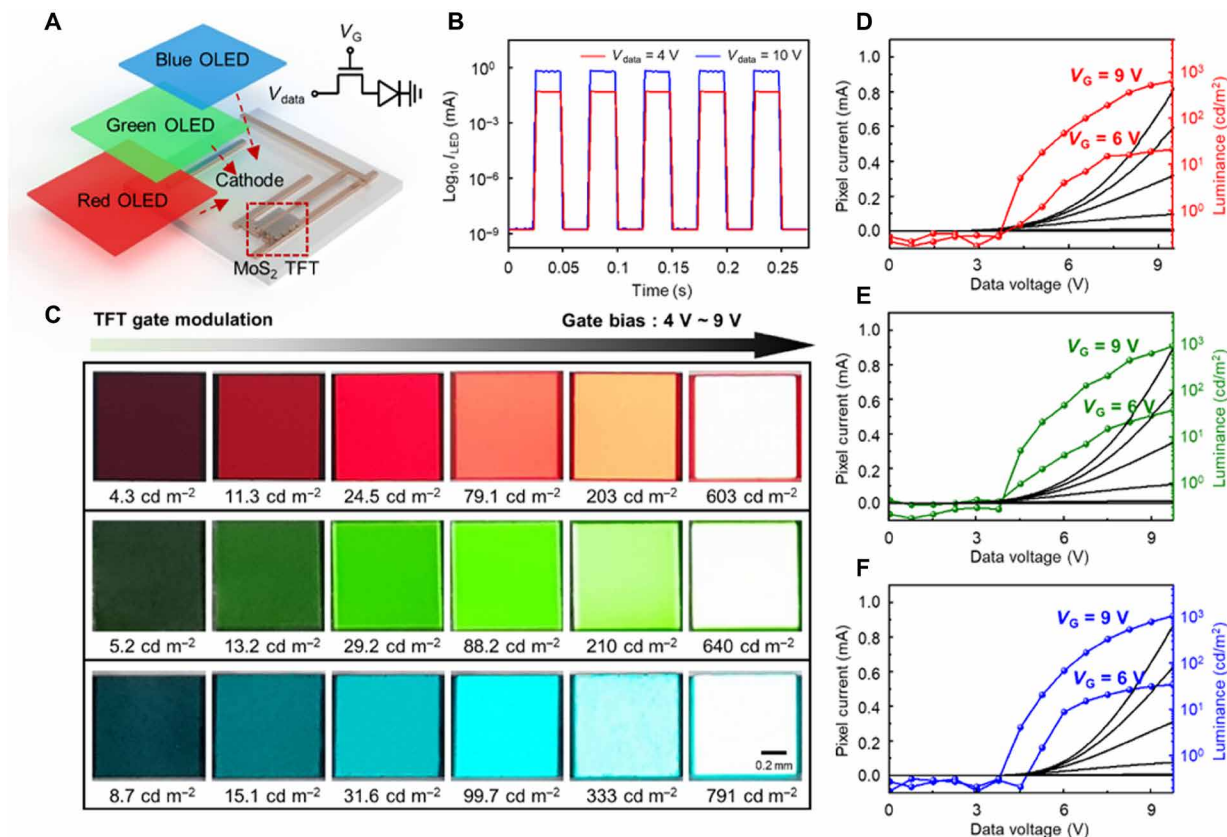


**Fig. 3. The properties of a single pixel integrated with the MoS<sub>2</sub> transistor and RGB OLEDs.** (A) Schematic illustration of the RGB unit pixel integrated with the MoS<sub>2</sub> transistor in a series connection for active-matrix configuration. (B) Pixel-switching properties controlled using a gate bias of  $-10$  and  $10$  V at fixed data biases of  $4$  V (red) and  $10$  V (blue). (C) Digital photograph of the luminance change in the RGB OLEDs in a gate bias range of  $4$  to  $9$  V, where the brightness of each OLED was stable and controlled by the gate signal of the MoS<sub>2</sub> transistor. (D to F) The pixel current (left y axis) and luminance (right y axis) as a function of gate signal. Photo credit: Sa-Rang Bae, Korea University.

that a single pixel was capable of operating within the large-area full-color AMOLED. The electroluminescence (EL) spectra of the RGB OLED pixels revealed that the highest luminance was measured at 460, 530, and 650 nm for the blue, green, and red OLEDs, respectively (Fig. 2G).

Large-area AMOLEDs on ultrathin PET substrates were produced using the high-performance MoS<sub>2</sub> backplane arrays and RGB OLEDs (Fig. 3A). As the backplane included an AMOLED, the OLED pixels operated via bottom emission. The OLED exhibited a rapid transition between the on and off states at a repeated gate pulse bias of  $\pm 10$  V (Fig. 3B), where the pulse response time was estimated to be 2.5 ms. While the response time was limited by the measurement system, the delay time was short. The observation of a single OLED demonstrated that the top-gate-configured MoS<sub>2</sub> TFT successfully operated the OLED unit. The emission intensity of the OLED measured between a  $V_{GS}$  of 4 and 9 V (1-V intervals) at a constant  $V_{DS}$  of 9 V indicated good operation of the MoS<sub>2</sub> TFT, where the luminance of the red OLED pixel was 4.3, 11.3, 24.5, 79.1, 203, and 603 cd/m<sup>2</sup>; the green OLED pixel was 5.2 to 13.2, 29.2, 88.2, 210, and 640 cd/m<sup>2</sup>; and the blue OLED pixel was 8.7 to 15.1, 31.6, 99.7, 333, and 791 cd/m<sup>2</sup> at a voltage of 4, 5, 6, 7, 8, and 9 V, respectively (Fig. 3C). The OLED current increased across the data voltage ( $V_{data}$ ) range at gate bias ( $V_G$ ) values of 6 and 9 V, and this was related to the difference in luminance at the two  $V_G$  values (Fig. 3, D to F). Gate modulation did not occur in the off state,

and the pixel current remained stable, indicating that the TFT operated without any leakage. The pixel current increased dramatically with increasing  $V_G$  in the on state. The threshold voltage of the OLEDs was 5 V during RGB pixel modulation, regardless of color type.

The performance of the individual RGB pixels using the MoS<sub>2</sub> transistors was confirmed, and an 18 by 18 array (324 pixels) was integrated to the data and gate lines of the MoS<sub>2</sub> transistor backplane circuitry, thus producing a full-color AMOLED display (fig. S6). Each pixel was individually controlled via the matrix line (Fig. 4A). Maintaining a consistent light luminance in each individual pixel is important in OLED display applications. The RGB OLED pixels in the display exhibited consistent and uniform brightness, even across the large area, because of the stable control of the gate and data signals. Each pixel operated according to the  $V_{data}$  value of the unit transistor when the  $V_G$  was fixed (23). The RGB pixel arrays were sequentially driven via the external drive circuit, which was configured in a commercialized strip pixel structure (Fig. 4B). The characters “R,” “G,” and “B” were clearly displayed on the external circuits, confirming that the RGB OLED pixels were controlled by the large-area MoS<sub>2</sub> backplane arrays to allow for full-color display operations (movie S1). Moreover, ultrathin device substrates are expected to enable the integration of the display on unusual foreign substrates (e.g., human hand) in wearable display applications. The operation of the device was stable, and the low stiffness of the ultrathin device system prevented deterioration of the optical and electrical properties during

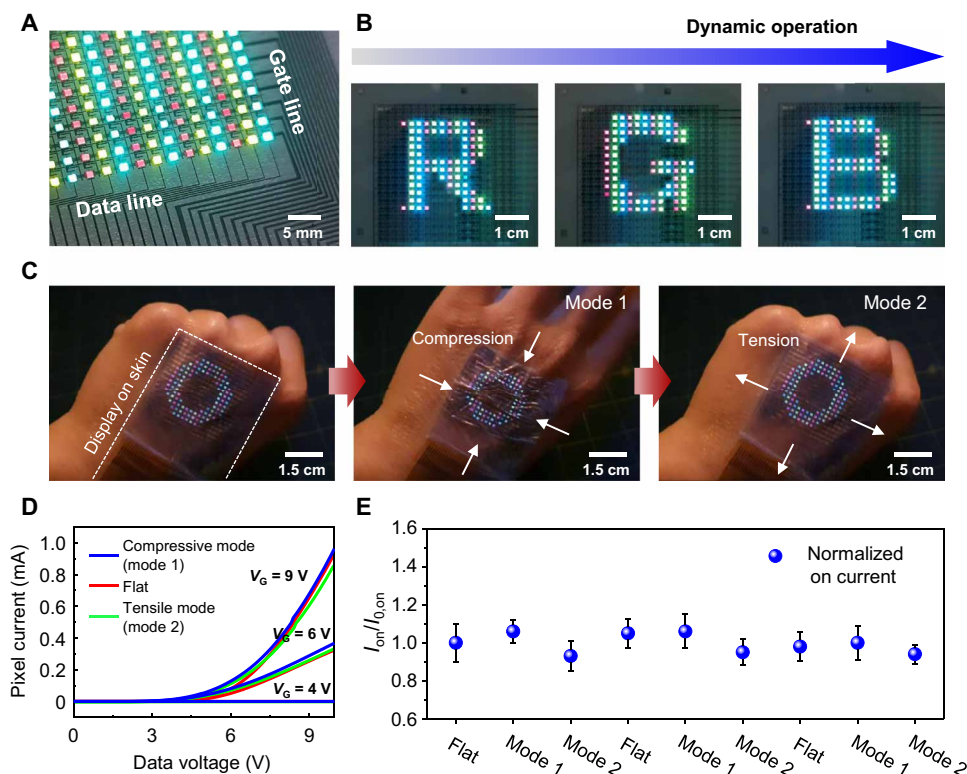


**Fig. 4. Wearable full-color AMOLED display based on MoS<sub>2</sub> backplane circuitry.** Digital photographs of the full-color active-matrix display during (A) the “all on” state; (B) the dynamic operation of the active-matrix display, where gate and data signals were individually controlled using the external circuit; and (C) the application of the ultrathin display on a human hand, where the display was deformed by two mechanical modes based on hand motion, namely, compressive mode (center) and tensile mode (right). (D) Plots of the unit pixel current as a function of data voltage at  $V_G$  values of 4 V (off state), 6 V, and 9 V in the compressive (blue), flat (red), and tensile (green) mode. At every applied gate bias ( $V_G$ ), negligible change in pixel current is observed under various modes of deformation, which enables stable operation of AMOLED on human hand. (E) Normalized on-state current variation of the ultrathin display on human hand during mechanical deformation. Photo credit: Minwoo Choi, Yonsei University.

substantial mechanical deformation (Fig. 4C and fig. S7) (19). A hand moves via two mechanical modes, the compressive mode (mode 1) and tensile mode (mode 2). Compressive stress in mode 1 can cause skin shrinkage and, in turn, random wrinkles on the device, while tensile stress in mode 2 can stretch the skin and affect the device (5). The current-voltage (*I-V*) characteristics indicated that the current level did not change substantially between lying flat (flat mode), mode 1, and mode 2 (Fig. 4D and movie S2). The detailed mechanical properties of the display were investigated by calculating normalized current levels based on the *I-V* characteristics. The on-state current did not fluctuate, and the variation below ca. 8% was acceptable for active-matrix display operation (Fig. 4E). Although the stability of the device was not yet perfect, we believe that it can be improved through further engineering work, and the MoS<sub>2</sub> transistor showed promise for practical application as a wearable full-color AMOLED display.

## DISCUSSION

A 2-inch, wearable full-color AMOLED display comprising 18-by-18 arrays was produced using MoS<sub>2</sub>-based backplane TFTs. The transistor array was built directly on a bilayer MoS<sub>2</sub> film grown using MOCVD. A high carrier mobility ( $>18 \text{ cm}^2 \text{ V}^{-1} \text{ s}^{-1}$ ) and on/off ratio ( $>10^7$ ) were observed, and the light emission of the RGB OLED pixels was controlled by applying a  $V_G$  between 4 and 9 V. The direct fabrication using an ultrathin plastic substrate combined with 2D semiconducting materials and OLED resulted in excellent electrical, optical, and mechanical performance and may be used in the development of future wearable electronic applications that would not be possible using conventional rigid inorganic materials.

## MATERIALS AND METHODS

### Synthesis of MoS<sub>2</sub>

MoS<sub>2</sub> growth was conducted in a hot-wall MOCVD system. A 4-inch Si substrate coated with SiO<sub>2</sub> (300 nm) was cleaned using acetone, isopropanol (IPA), and deionized water and dried in N<sub>2</sub> gas before use. The Si substrate was placed in the center of the furnace and held vertically at 90°. A plate containing NaCl grains was placed upstream to control the MoS<sub>2</sub> grain size. Molybdenum hexacarbonyl (MHC; Alfa Aesar, 13057) and dimethyl sulfide anhydrous (DMS; Sigma-Aldrich, 274380) were used as the Mo and S precursors, respectively, and were stored in glass bubblers outside the furnace to precisely control the amounts. Silica beads (ca. 2 mm) were added into the MHC bubbler for dehumidification. The system was evacuated to complete vacuum for 1 hour. The furnace was subsequently heated to 580°C under a mixture of 300 sccm (standard cubic centimeters per minute) Ar and 5 sccm H<sub>2</sub>, and the pressure was maintained at 10.0 torr. The flow rates of precursors were 1.0 sccm MHC and 0.6 sccm DMS, and MoS<sub>2</sub> growth was conducted for 24 hours to obtain a continuous MoS<sub>2</sub> film. The film was cooled to room temperature under an Ar environment.

### Fabrication of wearable full-color AMOLED display

A MoS<sub>2</sub>-based display backplane was fabricated on ultrathin PET (6 μm) attached to a carrier substrate that had been cleaned with acetone, IPA, and water. A bottom Al<sub>2</sub>O<sub>3</sub> layer (30 nm) was deposited using ALD. Source-drain electrodes (Cr/Au: 3/30 nm) for the TFTs were defined using standard photolithography at a width/length ratio of 300/4 μm. The bilayer MoS<sub>2</sub> film was transferred from the Si substrate

to the PET substrate, and the surface was patterned via reactive ion etching using CHF<sub>3</sub>/O<sub>2</sub> plasma. A top Al<sub>2</sub>O<sub>3</sub> layer (50 nm) was deposited to act as a dielectric layer for the TFTs. The device was annealed at 110°C in vacuum for 6 hours to prevent the formation of H<sub>2</sub>O molecule traps between the MoS<sub>2</sub> and Al<sub>2</sub>O<sub>3</sub> interface. The top-gate electrode was patterned using photolithography and a lift-off process. RGB OLEDs were deposited via vacuum deposition, and the device is transferred from the carrier substrate to a human hand. The skin is pre-stretched and followed by the attachment of AMOLED display onto the skin surface with the liquid bandage (Nexcare, 3M). The wearable AMOLED display was operated via a programmed external circuit.

### Fabrication of RGB OLEDs

OLEDs were manufactured on glass and flexible substrates. Indium tin oxide (ITO)-coated glass was washed with acetone, isopropyl alcohol, and deionized water; dried; and subjected to ultraviolet/ozone treatment for 15 min. Poly(3,4-ethylenedioxythiophene):poly(styrene sulfonate) was annealed at 150°C for 15 min after spin coating. The following materials were sequentially deposited to form the various OLEDs:

- 1) Green:
  - a) *N,N*-Di(1-naphthyl)-*N,N*-diphenyl-(1,10-biphenyl)-4,4-diamine (NPB, 40 nm)
  - b) Tris-(8-hydroxyquinoline)-aluminum (Alq<sub>3</sub>, 30 nm)
  - c) 10-(2-Benzothiazolyl)-2,3,6,7-tetrahydro-1,1,7,7-tetramethyl-1*H*,5*H*,11*H*-(1)benzo-pyropyrano(6,7-8-*I*,*j*)quinolizin-11-one (C545T, 5% doping)
  - d) Bathocuproine (BCP; 5 nm)
  - e) Tris-(8-hydroxy-quinoline) aluminum (Alq<sub>3</sub>, 25 nm)
- 2) Blue:
  - a) NPB (30 nm)
  - b) 9,9'-(1,3-Phenylene)bis-9*H*-carbazole (mCP, 30 nm) doped with bis[2-(4,6-difluorophenyl)pyridinato-C<sup>2</sup>,N](picolinato)iridium(III) (FIrpic, 10% doping)
  - c) BCP (20 nm)
- 3) Red:
  - a) NPB (40 nm)
  - b) Tris(4-carbazoyl-9-ylphenyl)amine (TCTA, 10 nm)
  - c) TCTA (20 nm) doped with tris(4-carbazoyl-9-ylphenyl)amine bis [2-(1-isoquinoliyl-*N*)phenyl-C] (2, 4-pentanedionato-O<sub>2</sub>, O<sub>4</sub>) iridium(III) [Ir(piq)<sub>2</sub>, 5% doping]
  - d) 3,3'-(5'-[3-(3-Pyridinyl)phenyl][1,1':3',1''-terphenyl]-3,3''-diyl) bispyridine (TmPyPB, 27 nm)

Lithium fluoride (LiF, 1 nm) and aluminum (Al, 100 nm) layers were thermally deposited to finish the OLEDs. A base pressure as low as 10<sup>-6</sup> torr was maintained within the chamber. The active area of the device was 0.5 mm × 0.5 mm.

### SUPPLEMENTARY MATERIALS

Supplementary material for this article is available at <http://advances.sciencemag.org/cgi/content/full/6/28/eabb5898/DC1>

### REFERENCES AND NOTES

1. C. Larson, B. Peele, S. Li, S. Robinson, M. Totaro, L. Beccai, B. Mazzolai, R. Shepherd, Highly stretchable electroluminescent skin for optical signaling and tactile sensing. *Science* **351**, 1071–1074 (2016).
2. T. Sekitani, H. Nakajima, H. Maeda, T. Fukushima, T. Aida, K. Hata, T. Someya, Stretchable active-matrix organic light-emitting diode display using printable elastic conductors. *Nat. Mater.* **8**, 494–499 (2009).

3. C. Wang, D. Hwang, Z. Yu, K. Takeji, J. Park, T. Chen, B. Ma, A. Javey, User-interactive electronic skin for instantaneous pressure visualization. *Nat. Mater.* **12**, 899–904 (2013).
4. G. H. Gelinck, H. E. A. Huitema, E. van Veenendaal, E. Cantatore, L. Schrijnemakers, J. B. P. H. van der Putten, T. C. T. Geuns, M. Beenhakkers, J. B. Giesbers, B.-H. Huisman, E. J. Meijer, E. M. Benito, F. J. Touwslager, A. W. Marsman, B. J. E. van Rens, D. M. de Leeuw, Flexible active-matrix displays and shift registers based on solution-processed organic transistors. *Nat. Mater.* **3**, 106–110 (2004).
5. M. Choi, B. Jang, W. Lee, S. Lee, T. W. Kim, H.-J. Lee, J.-H. Kim, J.-H. Ahn, Stretchable active matrix inorganic light-emitting diode display enabled by overlay-aligned roll-transfer printing. *Adv. Func. Mater.* **27**, 1606005 (2017).
6. Z. Bao, Materials and fabrication needs for low-cost organic transistor circuits. *Adv. Mater.* **12**, 227–230 (2000).
7. K. Liu, Q. Yan, M. Chen, W. Fan, Y. Sun, J. Suh, D. Fu, S. Lee, J. Zhou, S. Tongay, J. Ji, J. B. Neaton, J. Wu, Elastic properties of chemical-vapor-deposited monolayer MoS<sub>2</sub>, WS<sub>2</sub>, and their bilayer heterostructures. *Nano Lett.* **14**, 5097–5103 (2014).
8. G.-H. Lee, Y.-J. Yu, X. Cui, N. Petrone, C.-H. Lee, M. S. Choi, D.-Y. Lee, C. Lee, W. J. Yoo, K. Watanabe, T. Taniguchi, C. Nuckolls, P. Kim, J. Hone, Flexible and transparent MoS<sub>2</sub> field-effect transistors on hexagonal boron nitride-graphene heterostructures. *ACS Nano* **7**, 7931–7936 (2013).
9. K. Kang, S. Xie, L. Huang, Y. Han, P. Y. Huang, K. F. Mak, C.-J. Kim, D. Muller, J. Park, High-mobility three-atom-thick semiconducting films with wafer-scale homogeneity. *Nature* **520**, 656–660 (2015).
10. D. Jariwala, V. K. Sangwan, L. J. Lauhon, T. J. Marks, M. C. Hersam, Emerging device applications for semiconducting two-dimensional transition metal dichalcogenides. *ACS Nano* **8**, 1102–1120 (2014).
11. Y. Wang, J. C. Kim, R. J. Wu, J. Martinez, X. Song, J. Yang, F. Zhao, A. Mkhoyan, H. Y. Jeong, M. Chhowalla, Van der Waals contacts between three-dimensional metals and two-dimensional semiconductors. *Nature* **568**, 70–74 (2019).
12. S. Yu, J. S. Kim, P. J. Jeon, J. Ahn, J. C. Park, S. Im, Transition metal dichalcogenide-based transistor circuits for gray scale organic light-emitting displays. *Adv. Func. Mater.* **27**, 1603682 (2017).
13. M. Choi, Y. J. Park, B. K. Sharma, S.-R. Bae, S. Y. Kim, J.-H. Ahn, Flexible active-matrix organic light-emitting diode display enabled by MoS<sub>2</sub> thin-film transistor. *Sci. Adv.* **4**, eaas8721 (2018).
14. H. Yu, D. Liao, M. B. Johnston, B. Li, All-optical full-color displays using polymer nanofibers. *ACS Nano* **5**, 2020–2025 (2011).
15. M. C. Gather, A. Köhnen, A. Falcou, H. Becker, K. Meerholz, Solution-processed full-color polymer organic light-emitting diode displays fabricated by direct photolithography. *Adv. Func. Mater.* **17**, 191–200 (2007).
16. S. Li, B. N. Peele, C. M. Larson, H. Zhao, R. F. Shepherd, A stretchable multicolor display and touch interface using photopatterning and transfer printing. *Adv. Mater.* **28**, 9770–9775 (2016).
17. T.-H. Kim, K.-S. Cho, E. K. Lee, S. J. Lee, J. Chae, J. W. Kim, D. H. Kim, J.-Y. Kwon, G. Amaratunga, S. Y. Lee, B. L. Choi, Y. Kuk, J. M. Kim, K. Kim, Full-colour quantum dot displays fabricated by transfer printing. *Nat. Photonics* **5**, 176–182 (2011).
18. M. F. Reynolds, M. H. D. Guimarães, H. Gao, K. Kang, A. J. Cortese, D. C. Ralph, J. Park, P. L. McEuen, MoS<sub>2</sub> pixel arrays for real-time photoluminescence imaging of redox molecules. *Sci. Adv.* **5**, eaat9476 (2019).
19. Y. J. Park, B. K. Sharma, S. M. Shinde, M.-S. Kim, B. Jang, J.-H. Kim, J.-H. Ahn, All MoS<sub>2</sub>-based large area, skin-attachable active-matrix tactile sensor. *ACS Nano* **13**, 3023–3030 (2019).
20. Z. Lin, A. McCreary, N. Briggs, S. Subramanian, K. Zhang, Y. Sun, X. Li, N. J. Borys, H. Yuan, S. K. Fullerton-Shirey, A. Chernikov, H. Zhao, S. McDonnell, A. M. Lindenberg, K. Xiao, B. J. LeRoy, M. Drndić, J. C. M. Hwang, J. Park, M. Chhowalla, R. E. Schaak, A. Javey, M. C. Hersam, J. Robinson, M. Terrones, 2D materials advances: From large scale synthesis and controlled heterostructures to improved characterization techniques, defects and applications. *2D Mater.* **3**, 042001 (2016).
21. S. M. Shinde, T. Das, A. T. Hoang, B. K. Sharma, X. Chen, J.-H. Ahn, Surface-functionalization-mediated direct transfer of molybdenum disulfide for large-area flexible devices. *Adv. Func. Mater.* **28**, 1706231 (2018).
22. C. Wang, K. Sim, J. Chen, H. Kim, Z. Rao, Y. Li, W. Chen, J. Song, R. Verduzco, C. Yu, Soft ultrathin electronics innervated adaptive fully soft robots. *Adv. Mater.* **30**, e1706695 (2018).
23. M. A. McCarthy, B. Liu, E. P. Donoghue, I. Kravchenko, D. Y. Kim, F. So, A. G. Rinzler, Low-voltage, low-power, organic light-emitting transistors for active matrix displays. *Science* **332**, 570–573 (2011).

#### Acknowledgments

**Funding:** This work was supported by the National Research Foundation of Korea (NRF-2015R1A3A2066337 and 2018R1A4A1022647). **Author contributions:** J.-H.A. and S.Y.K. planned and supervised the project. M.C. and S.-R.B. conducted most of the device fabrication and characterization experiments. L.H. and A.T.H. supported the operation of OLED display and the synthesis of MoS<sub>2</sub>, respectively. All authors contributed to data analysis and manuscript writing. **Competing interests:** The authors declare that they have no competing interests. **Data and materials availability:** All data needed to evaluate the conclusions in the paper are present in the paper and/or the Supplementary Materials. Additional data related to this paper may be requested from the authors.

Submitted 5 March 2020

Accepted 27 May 2020

Published 8 July 2020

10.1126/sciadv.abb5898

**Citation:** M. Choi, S.-R. Bae, L. Hu, A. T. Hoang, S. Y. Kim, J.-H. Ahn, Full-color active-matrix organic light-emitting diode display on human skin based on a large-area MoS<sub>2</sub> backplane. *Sci. Adv.* **6**, eabb5898 (2020).

## Full-color active-matrix organic light-emitting diode display on human skin based on a large-area MoS<sub>2</sub> backplane

Minwoo Choi, Sa-Rang Bae, Luhing Hu, Anh Tuan Hoang, Soo Young Kim and Jong-Hyun Ahn

*Sci Adv* 6 (28), eabb5898.  
DOI: 10.1126/sciadv.abb5898

ARTICLE TOOLS	<a href="http://advances.sciencemag.org/content/6/28/eabb5898">http://advances.sciencemag.org/content/6/28/eabb5898</a>
SUPPLEMENTARY MATERIALS	<a href="http://advances.sciencemag.org/content/suppl/2020/07/06/6.28.eabb5898.DC1">http://advances.sciencemag.org/content/suppl/2020/07/06/6.28.eabb5898.DC1</a>
REFERENCES	This article cites 23 articles, 4 of which you can access for free <a href="http://advances.sciencemag.org/content/6/28/eabb5898#BIBL">http://advances.sciencemag.org/content/6/28/eabb5898#BIBL</a>
PERMISSIONS	<a href="http://www.sciencemag.org/help/reprints-and-permissions">http://www.sciencemag.org/help/reprints-and-permissions</a>

Use of this article is subject to the [Terms of Service](#)

---

*Science Advances* (ISSN 2375-2548) is published by the American Association for the Advancement of Science, 1200 New York Avenue NW, Washington, DC 20005. The title *Science Advances* is a registered trademark of AAAS.

Copyright © 2020 The Authors, some rights reserved; exclusive licensee American Association for the Advancement of Science. No claim to original U.S. Government Works. Distributed under a Creative Commons Attribution NonCommercial License 4.0 (CC BY-NC).